

Research Article

Investigation of Traffic Loading Effects for Different Codes on Medium- and Small-Span Girder Bridges in China

Qingfei Gao ¹, Biao Wu,¹ Jun Li,² Kemeng Cui,³ and Chuang Xu⁴

¹School of Transportation Science and Engineering, Harbin Institute of Technology, Harbin, Heilongjiang 150090, China

²Department of Municipal and Environmental Engineering, Heilongjiang Institute of Construction Technology, Harbin, Heilongjiang 150025, China

³School of Civil Engineering, Southeast University, Nanjing, Jiangsu 210096, China

⁴Heilongjiang Province Highway Survey and Design Institute, Harbin, Heilongjiang 150080, China

Correspondence should be addressed to Qingfei Gao; gaoqingfei@hit.edu.cn

Received 18 August 2020; Accepted 28 August 2020; Published 7 September 2020

Academic Editor: Yi Zhang

Copyright © 2020 Qingfei Gao et al. This is an open access article distributed under the Creative Commons Attribution License, which permits unrestricted use, distribution, and reproduction in any medium, provided the original work is properly cited.

With increasing traffic volume, the traffic load grade given by design codes has gradually increased. For new bridges, there is no problem, and the traffic load can be met through the requirements of the new code. However, for existing bridges, there is a lack of uniform standards on whether they can continue to be used. It is not clear whether these bridges will be judged according to the new code or the original design code. The traffic loading effects of different codes on medium- and small-span girder bridges in China are investigated in this study. Three codes are introduced: JTJ 021-89, JTG D60-2004, and JTG D60-2015. Simply supported girder bridges and continuous girder bridges are discussed. The traffic loading effects calculated based on JTG D60-2015 are significantly larger than those calculated based on JTJ 021-89. For simply supported girder bridges, most of the differences range from 20% to 40%, and the maximum value is almost larger than 60%. For continuous girder bridges, most of the differences in the positive bending moments are concentrated in the 20%~40% range, while the differences in the negative bending moments range from 10% to 20%. Therefore, the differences in traffic loading effects calculated based on various codes cannot be ignored in actual bridge engineering. The conclusion in this study can provide a basis for bridge structure evaluation and life prediction.

1. Introduction

Bridges are one of the most important civil structures. By the end of 2019, approximately 878300 highway bridges were built in China; most of them were medium- and small-span girder bridges [1]. For medium- and small-span girder bridges, the ratio between a dead load and a live load is relatively small, which means that a live load has a greater influence on bridges.

With increasing traffic volume, the traffic load grade given by the code increases gradually [2]. For new bridges, there is no problem, and the traffic load can be met through the requirements of the new code. However, for existing bridges, there is a lack of uniform standards on whether they can continue to be used, and it is not clear whether these bridges will be judged according to the new code or the

original design code. Different from other civil structures, the traffic load is the most important load. The design life of the bridge is 100 years. However, the design code is revised once every ten or twenty years. In other words, for existing bridges, the traffic volume in the new code is larger, sometimes overloading.

To ensure the safety of bridges, monitoring and inspection are two important measures. A structure healthy monitoring system plays a vital role in bridge safety [3–5]. However, the system is only installed in some large-span bridges due to its high cost. For medium- and small-span bridges, the inspection measure is much better, and a loading test is the main method of inspection. Whether the loading test should adopt the original design code or the current code has not always been agreed upon and has been used at will [6, 7].

The differences among various codes have been investigated by many researchers [8–14]; however, most of them have focused on early codes and simply supported girder bridges. Additionally, compared with simply supported girder bridges, there are more continuous girder bridges [15]. Structural reliability-based live load factors have been developed by truck load effect statistics using the analytical model of the platoons of trucks and the extrapolation approach, taking a number of temporal maximum values [16]. The characterization of live load models is of paramount importance for an accurate evaluation of the structural safety and reliability of bridges and the calibration of design loads for use when designing new bridges or assessing the safety of existing bridges [17–20].

Traffic loading effects in different codes on medium- and small-span girder bridges in China are investigated in this study. Three codes are introduced including JTJ 021-89 [21], JTG D60-2004 [22], and JTG D60-2015 [23]. Simply supported girder bridges and continuous girder bridges are discussed.

2. Traffic Loads in Different Codes

Different from other civil engineering structures, moving vehicle loads are one of the main load forms of bridge structures. Because of the vehicle-bridge coupled vibration, the bridge response is larger when subjected to moving vehicles. Static traffic loads and dynamic load allowances in different codes are introduced in this section.

2.1. Static Traffic Loads in Different Codes. During the last 40 years, there have been three versions of the traffic load code in China: JTJ 021-89, JTG D60-2004, and JTG D60-2015.

In JTJ 021-89, the traffic load is simulated as one loading truck and multistandard cars. There are four types of the traffic load grades including traffic-over 20, traffic-20, traffic-15, and traffic-10. In addition, different traffic load grades are applied for various highway grades. The corresponding relation in JTJ 021-89 is shown in Table 1, and the details of different traffic load grades are shown in Figure 1.

The traffic load modes are more similar to the actual situation. However, these models are not convenient for manual and computer loading, and the calculation effect is discontinuous with the variation in bridge spans. Therefore, the model has been replaced by a computational scheme consisting of the uniform force q_k and the concentrated force P_k in JTG D60-2004, as shown in Figure 2. According to the calculation scheme, the load effect can be calculated as long as the influence line area and the maximum vertical coordinate value of the bridge are known.

In JTG D60-2004, the traffic loads are reduced to two grades: highway-grade I and highway-grade II. Highway-grade I in JTG D60-2004 is similar to traffic-over 20 in JTJ 021-89, while highway-grade II is similar to traffic-20. With the rapid development of society, the vehicle load is larger, and traffic-15 and traffic-10 are no longer used. The corresponding relation in JTG D60-2004 is shown in Table 2.

The traffic loads in JTG D60-2004 are fictitious. The uniform load q_k and the concentrated load P_k are deduced from various cases of different vehicle weights and spacings. For highway-grade I, the uniform load q_k is 10.5 kN/m, and the concentrated load P_k is calculated by equation (1). The uniform load q_k and concentrated load P_k of highway-grade II are adopted as 0.75 times those of highway-grade I.

$$P_k = \begin{cases} 180 \text{ (kN)}, & L \leq 5 \text{ m}, \\ 160 + 4L \text{ (kN)}, & 5 \text{ m} < L < 50 \text{ m}, \\ 360 \text{ (kN)}, & L \geq 50 \text{ m}, \end{cases} \quad (1)$$

where L is the span length of the bridge.

From 2008 to 2011, through an investigation and statistical analysis of the current situation of automobile loads in China, the automobile load variability increased considerably compared with that of the past. Due to the small proportion of the constant load and live load of medium- and small-span bridges, this variability has a great impact on small-span bridges. In practice, accidents caused by heavy load vehicles crushing bridges are mostly medium- and small-span bridges. In view of this, the revised code improves the standard value of the concentrated lane load of bridges under a 5 m span and increases the design load effect of bridges within a 50 m span. In detail, the concentrated load P_k is calculated by equation (2) in JTG D60-2015.

$$P_k = \begin{cases} 270 \text{ (kN)}, & L \leq 5 \text{ m}, \\ 260 + 2L \text{ (kN)}, & 5 \text{ m} < L < 50 \text{ m}, \\ 360 \text{ (kN)}, & L \geq 50 \text{ m}. \end{cases} \quad (2)$$

Since 2009, most toll collections on second-class highways have gradually been abolished in China, and the traffic volume and load level of some of these highways have increased considerably. Therefore, the specification adjusts the car load level of the second-class highway to highway-grade I. The corresponding relation in JTG D60-2015 is shown in Table 3.

By a comparison of different versions of the codes, it can be seen that the traffic load grade matched with the highway grade is gradually increasing, especially for a low-grade highway. In addition, even for the same traffic load grade, the specific value is improved. In short, the traffic load grade has been increasing.

2.2. Dynamic Load Allowances in Different Codes. The dynamic load allowance is the application factor of the dynamic responses of bridges subjected to moving vehicles [24, 25]. The impact effect is generally expressed via statics, which means that the dynamic effect of vehicle action is expressed by multiplying the gravity of a vehicle by the dynamic load allowance. Considerable research has been conducted on the expression of the dynamic load allowance.

In JTJ 021-89, the dynamic load allowance μ is expressed as a function of the bridge span length L , as shown in the following equation:

TABLE 1: Traffic load grades of the bridges in different highway grades in JTJ 021-89.

Highway grades	Expressway	First-class highway	Second-class highway	Third-class highway	Fourth-class highway
Traffic loads grades	Traffic-over 20	Traffic-over 20 Traffic-20	Traffic-20	Traffic-15	Traffic-10

Note: traffic-over 20 is applied for the first-class highway subjected to container transportation, while traffic-20 is applied for other cases.

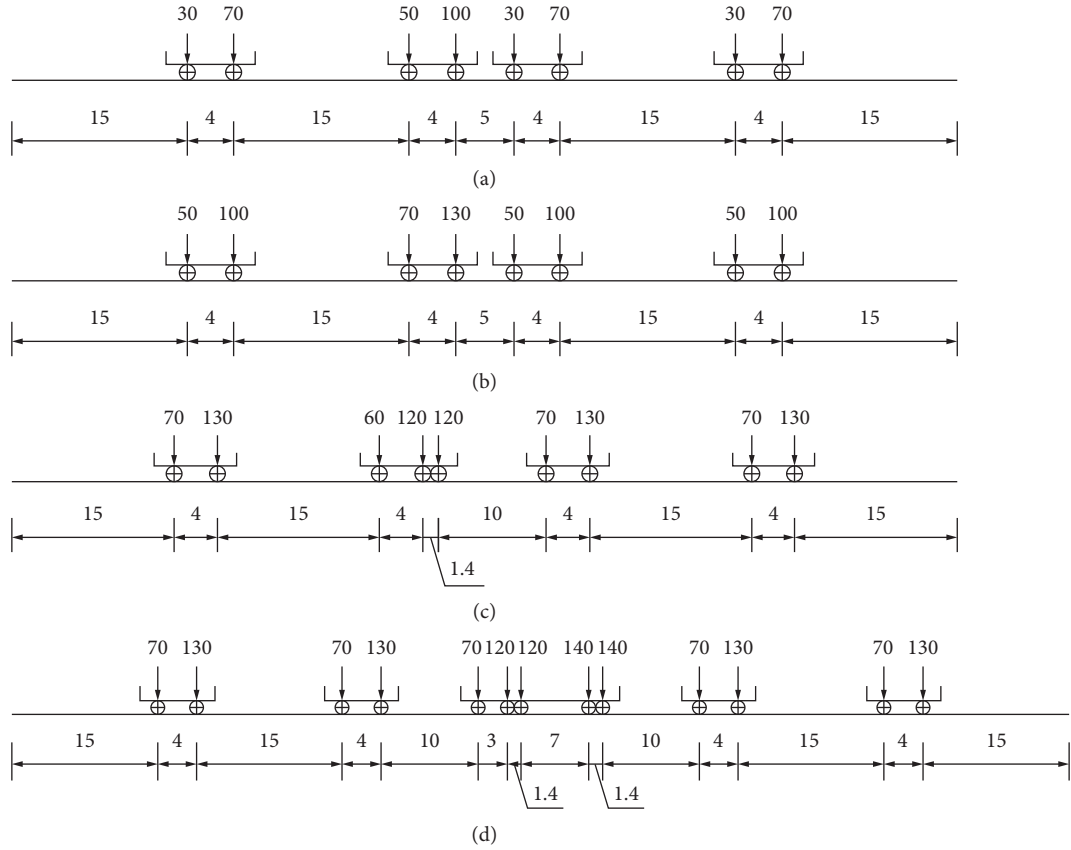


FIGURE 1: Different traffic load grades in JTJ 021-89: (a) traffic-10; (b) traffic-15; (c) traffic-20; (d) traffic-over 20.

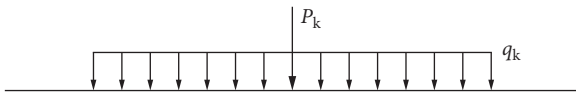


FIGURE 2: Different traffic load grades in JTG D60-2004.

$$\mu = \begin{cases} 0.30, & L \leq 5 \text{ m}, \\ \frac{0.30}{45 - 5} \times (45 - L), & 5 \text{ m} < L < 45 \text{ m}, \\ 0, & L \geq 45 \text{ m}. \end{cases} \quad (3)$$

However, the dynamic load allowance is more related to the fundamental frequency of the bridge. More than 6,600 representative samples of dynamic load allowances are collected from the measured data of seven bridges with different spans and initial conditions (from the rectangular reinforced concrete slab bridge with a 6 m span to the

prestressed concrete box girder bridge with a 45 m span) through a 12 h continuous observation by the dynamic test system. Through the estimation of statistical parameters and the goodness-of-fit test of the probability distribution, it is shown that all kinds of dynamic load allowances in different bridges do not reject the extreme value type I distribution. According to the common worldwide practice, a 95% guarantee rate is taken as the dynamic load allowance of highway bridges. Through regression analysis, the relation curve between the dynamic load allowance and the fundamental frequency of the bridge structure is obtained. After an appropriate correction, this value is adopted in JTG D60-2004 and JTG D60-2015, as shown in the following equation:

$$\mu = \begin{cases} 0.05, & f < 1.5 \text{ Hz}, \\ 0.1767 \ln f - 0.0157, & 1.5 \text{ Hz} \leq L \leq 14 \text{ Hz}, \\ 0.45, & f > 14 \text{ Hz}, \end{cases} \quad (4)$$

where f is the fundamental frequency of the bridge.

TABLE 2: Traffic load grades of the bridges for different highway grades in JTG D60-2004.

Highway grades	Expressway	First-class highway	Second-class highway	Third-class highway	Fourth-class highway
Traffic load grades	Highway-grade I	Highway-grade I	Highway-grade II	Highway-grade II	Highway-grade II

TABLE 3: Traffic load grades of the bridges for different highway grades in JTG D60-2015.

Highway grades	Expressway	First-class highway	Second-class highway	Third-class highway	Fourth-class highway
Traffic loads grades	Highway-grade I	Highway-grade I	Highway-grade I	Highway-grade II	Highway-grade II

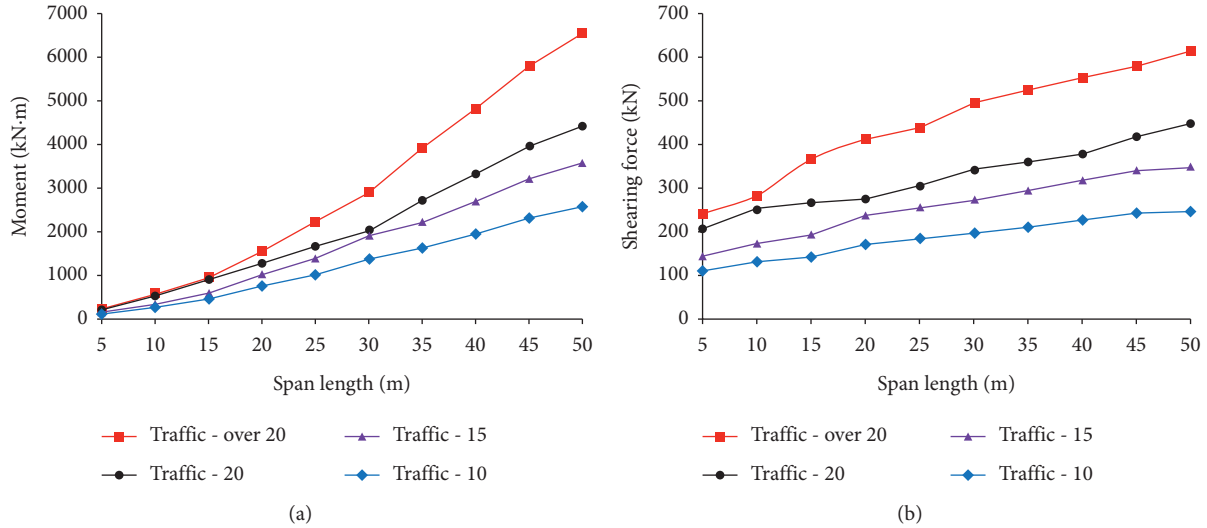


FIGURE 3: Traffic loading effects in JTJ 021-89: (a) moment and (b) shearing force.

Certainly, the traffic effects should be the product of the static traffic load effect and dynamic load allowance.

3. Simply Supported Girder Bridges

The structural characteristics of the simply supported girder bridge are clear, and its construction method is relatively simple. The common span range of a simply supported girder bridge is 5~40 m. In this paper, common simply supported girder bridges are selected. The main traffic loading effects in different codes are comparatively studied, including the bending moment in the midspan section and the shearing force in the pier-top section.

3.1. Different Traffic Loading Effects in Various Codes. The traffic loading effects in various codes are studied including JTJ 021-89, JTG D60-2004, and JTG D60-2015. The results are shown in Figures 3–5.

The bending moment and shearing force both increase with increasing span length. With increasing traffic load grades, the increase in the moment effect is more obvious than that of the shearing force effect. In addition, the overall variation trends of JTG D60-2004 and JTG D60-2015 are basically the same, but they are significantly different from JTJ 021-89, which is mainly caused by the large difference in traffic load models.

3.2. Traffic Loading Effects without Dynamic Load Allowance in Different Codes. As previously mentioned, highway-grade I in JTG D60-2004 and JTG D60-2015 is similar to traffic-over 20 in JTJ 021-89, while highway-grade II is similar to traffic-20. To more clearly compare the differences between the corresponding load grades in the different codes, highway-grade I and traffic-over 20 are referred to as class I loads, while highway-grade II and traffic-20 are referred to as class II loads. Additionally, three ratio parameters are introduced:

$$\begin{aligned}\eta_{S1} &= \frac{S_{JTG D60-2004} - S_{JTJ021-89}}{S_{JTJ021-89}}, \\ \eta_{S2} &= \frac{S_{JTG D60-2015} - S_{JTJ021-89}}{S_{JTJ021-89}}, \\ \eta_{S3} &= \frac{S_{JTG D60-2015} - S_{JTJ D60-2004}}{S_{JTJ D60-2004}},\end{aligned}\quad (5)$$

where $S_{JTJ 021-89}$ is the traffic loading effect calculated based on JTJ 021-89, $S_{JTG D60-2004}$ is the traffic loading effect calculated based on JTG D60-2004, and $S_{JTG D60-2015}$ is the traffic loading effect calculated based on JTG D60-2015.

A comparison of the traffic loading effects without a dynamic load allowance in different codes is shown in Figure 6. Legends Q-I and M-I indicate the shearing force of

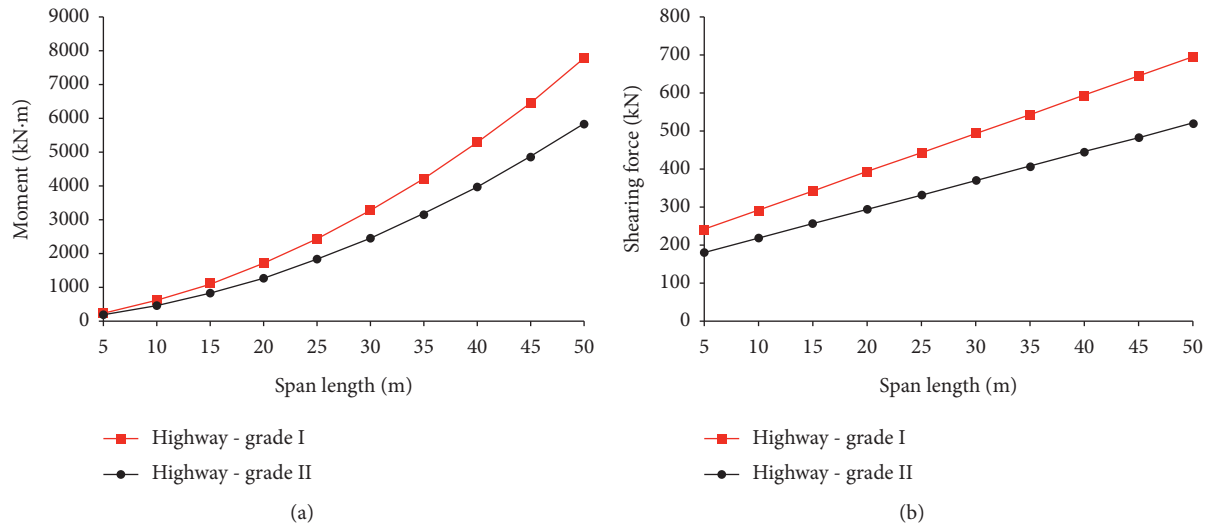


FIGURE 4: Traffic loading effects in JTGD60-2004: (a) moment and (b) shearing force.

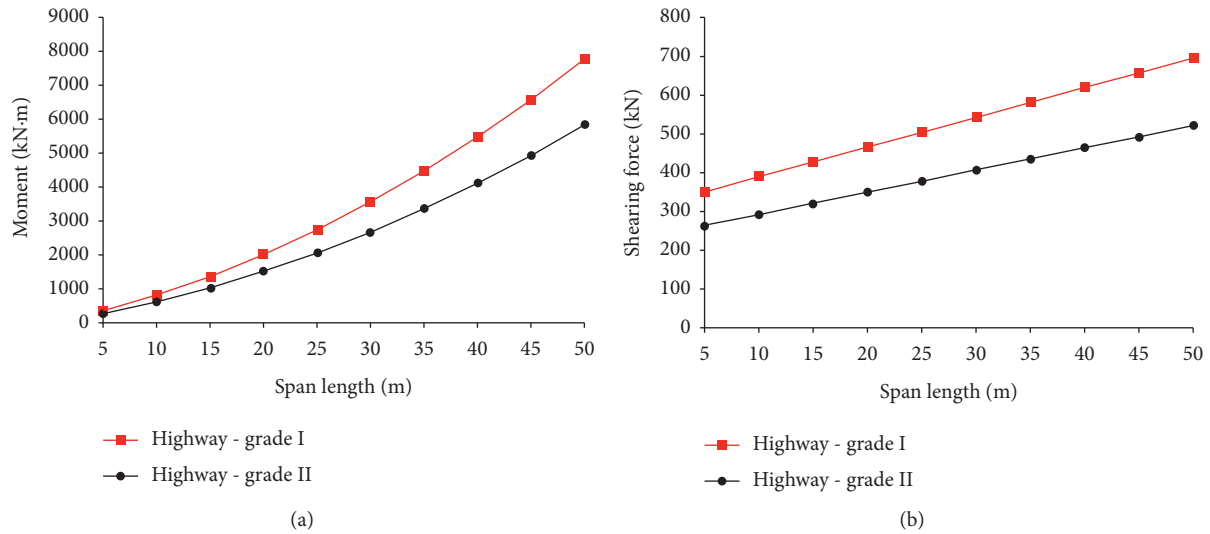


FIGURE 5: Traffic loading effects in JTGD60-2015: (a) moment and (b) shearing force.

the pier-top section and the bending moment of the midspan section induced by the class I load, while legends Q-II and M-II indicate the shearing force of the pier-top section and the bending moment of the midspan section induced by the class II load.

It can be seen from Figure 6(a) that, without a dynamic load allowance, there is little difference between the traffic loading effects calculated based on JTGD60-2004 and those calculated based on JTJ 021-89 when the span length of the simply supported girder bridge is less than 20 m. However, when the span is greater than 20 m, the effect will increase significantly, and the difference will be larger with increasing span length, but most of the differences range from 10% to 15%, and the influence is not very great. In addition, the difference in the bending moment induced by the class II load is larger.

Similarly, Figure 6(b) shows that all the traffic loading effects of the simply supported girder bridges calculated based on JTGD60-2015 are significantly larger than those

calculated based on JTJ 021-89, especially for small-span bridges. Most of the differences are concentrated in the 10%~25% range.

In Figure 6(c), the comparison of the traffic loading effects between JTGD60-2004 and JTGD60-2004 is very regular because their traffic loading models are similar, and only the value of the concentrated force P_k is different. The differences between them decrease with increasing span length. For small-span simply supported girder bridges, the difference can reach almost 45%, which should be given more attention in actual engineering.

3.3. Traffic Loading Effects with Dynamic Load Allowance in Different Codes. As previously mentioned, the traffic effects should be the product of the static traffic load effect and dynamic load allowance. The dynamic load allowance in JTGD60-2004 and JTGD60-2015 is the same but is different

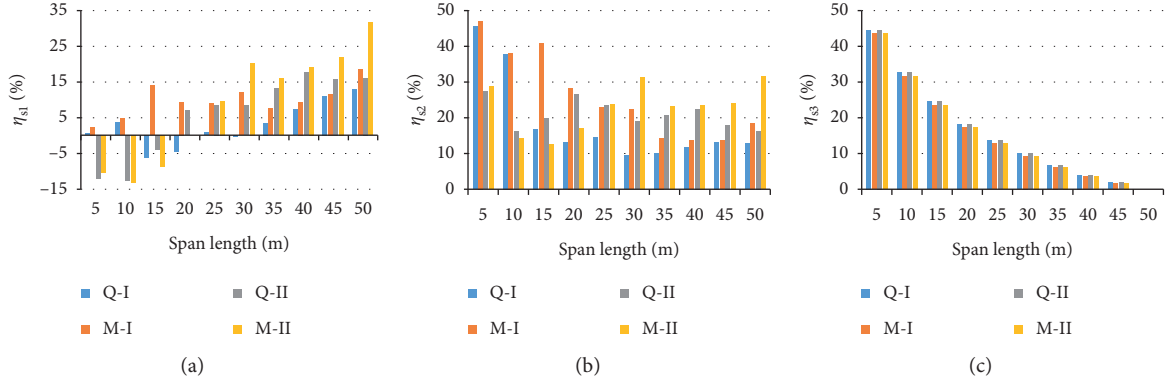


FIGURE 6: Comparison of the traffic loading effects without a dynamic load allowance: (a) η_{S1} ; (b) η_{S2} ; (c) η_{S3} .

from that in JTJ 021-89. Similarly, two ratio parameters are introduced:

$$\eta_{DS1} = \frac{SD_{JTG D60-2004} - SD_{JTJ021-89}}{SD_{JTJ021-89}}, \quad (6)$$

$$\eta_{DS2} = \frac{SD_{JTG D60-2015} - SD_{JTJ021-89}}{SD_{JTJ021-89}},$$

where $SD_{JTJ 021-89}$ is the traffic loading effect (including the dynamic load allowance) calculated based on JTJ 021-89, $SD_{JTG D60-2004}$ is the traffic loading effect (including the dynamic load allowance) calculated based on JTG D60-2004, and $SD_{JTG D60-2015}$ is the traffic loading effect (including the dynamic load allowance) calculated based on JTG D60-2015.

A comparison of the traffic loading effects with the dynamic load allowance in different codes is shown in Figure 7. Because the dynamic load allowances in JTG D60-2004 and JTG D60-2015 are the same, the comparison results of the traffic loading effects with the dynamic load allowance in these two codes are the same as in Figure 6(c) and will not be discussed again here.

Figure 7(a) shows that, with dynamic load allowance, the traffic loading effects of simply supported girder bridges calculated based on JTG D60-2015 are significantly larger than those calculated based on JTJ 021-89 when the span length is larger than 20 m. All the differences are larger than 10%. However, the comparison is not clear when the span length is less than 20 m.

Similarly, Figure 7(b) shows that all the traffic loading effects of the simply supported girder bridges calculated based on JTG D60-2015 are significantly larger than those calculated based on JTJ 021-89, especially for small-span bridges. Most of the differences range from 20% to 40%, and the maximum value is almost larger than 60%.

In other words, for simply supported girder bridges, the differences in traffic loading effects calculated based on various codes cannot be ignored in actual bridge engineering, especially for small-span bridges.

4. Continuous Girder Bridges

Although the construction of simply supported girder bridges is simple, the driving comfort is poor due to the large

number of expansion joints. In addition, compared with a simply supported girder bridge, the pier-top section of a continuous girder bridge bears a negative bending moment, which will share a positive bending moment in the midspan section, and the stress is more reasonable. Therefore, with the progress of construction technology and the improvement in people's living standards, continuous girder bridges are more common.

Similarly, without the dynamic load allowance, three ratio parameters for continuous girder bridges are introduced:

$$\eta_{C1} = \frac{C_{JTG D60-2004} - C_{JTJ021-89}}{C_{JTJ021-89}},$$

$$\eta_{C2} = \frac{C_{JTG D60-2015} - C_{JTJ021-89}}{C_{JTJ021-89}}, \quad (7)$$

$$\eta_{C3} = \frac{C_{JTG D60-2015} - C_{JTG D60-2004}}{C_{JTG D60-2004}},$$

where $C_{JTJ 021-89}$ is the traffic loading effect of continuous girder bridges calculated based on JTJ 021-89, $C_{JTG D60-2004}$ is the traffic loading effect of continuous girder bridges calculated based on JTG D60-2004, and $C_{JTG D60-2015}$ is the traffic loading effect of continuous girder bridges calculated based on JTG D60-2015.

With the dynamic load allowance, two ratio parameters for continuous girder bridges are introduced:

$$\eta_{DC1} = \frac{CD_{JTG D60-2004} - CD_{JTJ021-89}}{CD_{JTJ021-89}}, \quad (8)$$

$$\eta_{DC2} = \frac{CD_{JTG D60-2015} - CD_{JTJ021-89}}{CD_{JTJ021-89}},$$

where $CD_{JTJ 021-89}$ is the traffic loading effect (including the dynamic load allowance) of continuous girder bridges calculated based on JTJ 021-89, $CD_{JTG D60-2004}$ is the traffic loading effect (including the dynamic load allowance) of continuous girder bridges calculated based on JTG D60-2004, and $CD_{JTG D60-2015}$ is the traffic loading effect (including the dynamic load allowance) of continuous girder bridges calculated based on JTG D60-2015.

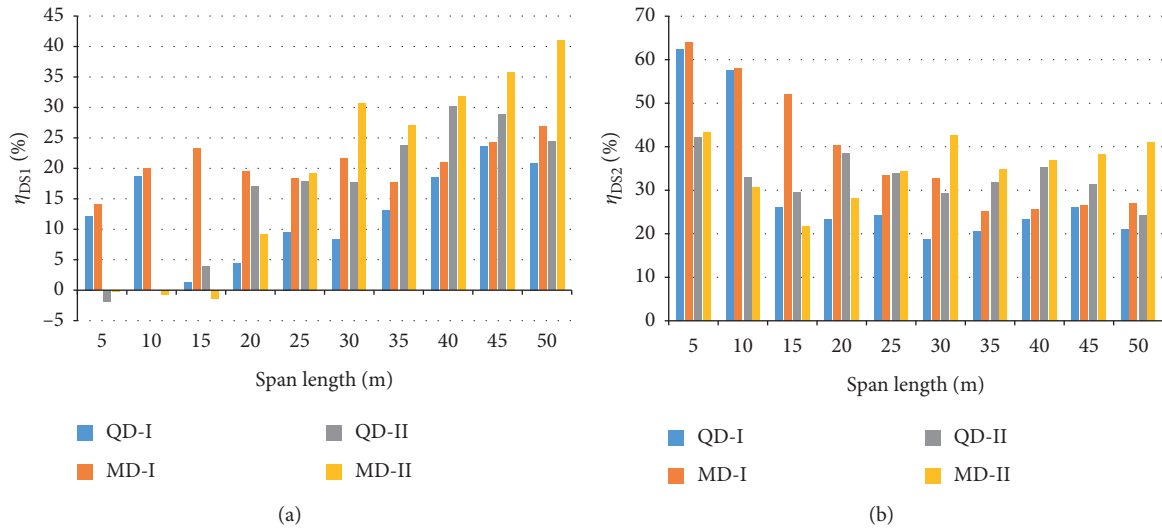


FIGURE 7: Comparison of the traffic loading effects with the dynamic load allowance: (a) η_{DS1} and (b) η_{DS2} .

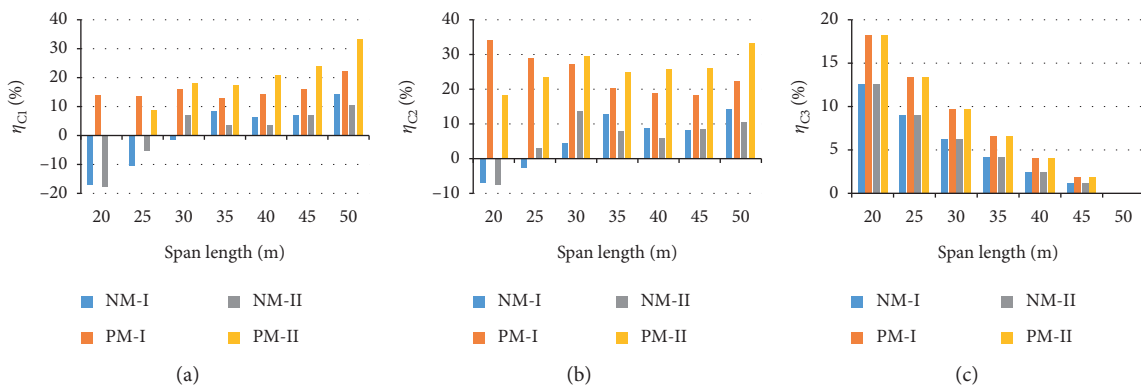


FIGURE 8: Comparison of the traffic loading effects of three-span continuous girder bridges without the dynamic load allowance: (a) η_{C1} ; (b) η_{C2} ; (c) η_{C3} .

Considering the telescopic deformation caused by the influence of temperature, the span number of common continuous girder bridges ranges from three to five. Therefore, in this paper, continuous girder bridges with 3~5 spans are studied. For continuous girder bridges, the negative bending moment in the pier-top section and the positive bending moment in the midspan section are the focus.

4.1. Three-Span Continuous Girder Bridges. The comparison results of the traffic loading effects of three-span continuous girder bridges without a dynamic load allowance are shown in Figure 8. Legends NM-I and PM-I indicate the negative bending moment of the pier-top section and the positive bending moment of the midspan section induced by the class I load, while legends NM-II and PM-II indicate the negative bending moment of the pier-top section and the positive bending moment of the midspan section induced by the class II load.

Figure 8(a) shows that the negative bending moment calculated based on JTG D60-2004 is smaller than that calculated based on JTJ 021-89 when the span length is less than 30 m, while the negative bending moment calculated based on JTG D60-2004 is larger than that calculated based on JTJ 021-89 when the span length is longer than 30 m. In addition, the positive bending moment calculated based on JTG D60-2004 is significantly larger than that calculated based on JTJ 021-89. The differences between them ranged from almost 10% to 20%.

Similarly, it can be seen from Figure 8(b) that the trend of the negative bending moment is almost the same as that in Figure 8(a). However, the positive bending moment calculated based on JTG D60-2004 is significantly larger than that calculated based on JTJ 021-89. Most of the differences range from 15% to 30%, and the largest difference is 35%.

In Figure 8(c), the comparison of the traffic loading effects between JTG D60-2004 and JTG D60-2004 is very regular because their traffic loading models are similar, and

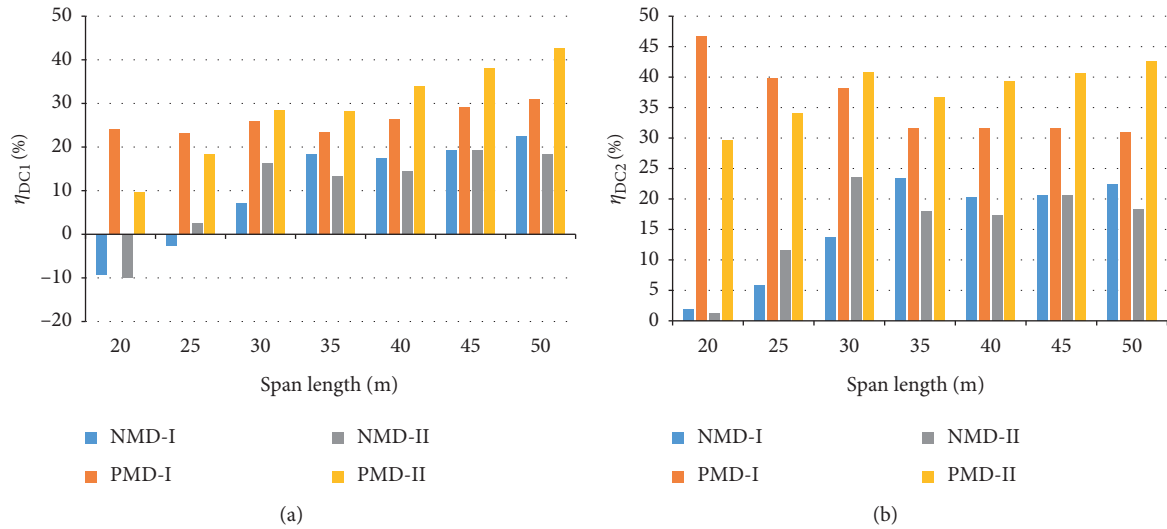


FIGURE 9: Comparison of the traffic loading effects of three-span continuous girder bridges with the dynamic load allowance: (a) η_{DC1} and (b) η_{DC2} .

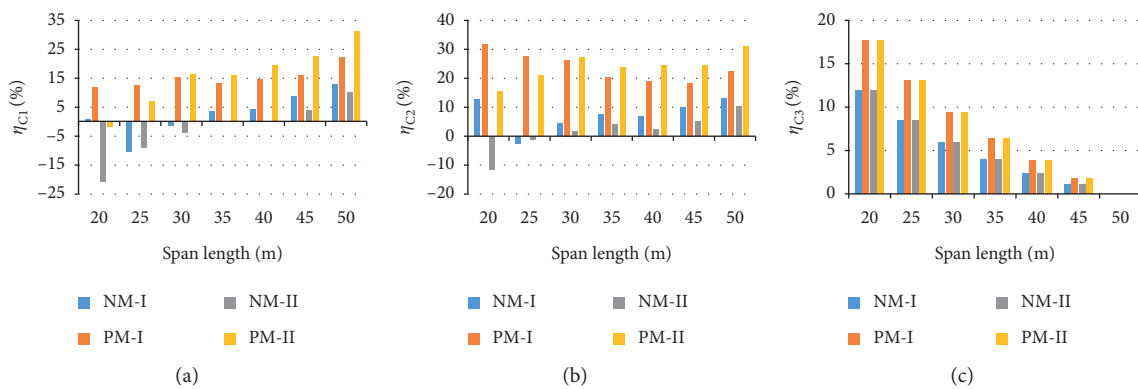


FIGURE 10: Comparison of the traffic loading effects of four-span continuous girder bridges without the dynamic load allowance: (a) η_{C1} ; (b) η_{C2} ; (c) η_{C3} .

only the value of the concentrated force P_k is different. The differences between these values decrease with increasing span length. For small-span continuous girder bridges, the difference can reach almost 18% and 12% for the positive bending moment and negative bending moment, respectively.

A comparison of the traffic loading effects of three-span continuous girder bridges with the dynamic load allowance in different codes is shown in Figure 9.

Figure 9(a) shows that, with the dynamic load allowance, the positive bending moments of three-span continuous girder bridges calculated based on JTG D60-2015 are significantly larger than those calculated based on JTJ 021-89. The differences in the positive bending moment are larger than 20%. In addition, the largest difference in the negative bending moment can reach 22%.

Similarly, it can be seen from Figure 9(b) that all the traffic loading effects of the three-span continuous girder bridges calculated based on JTG D60-2015 are significantly larger than those calculated based on JTJ 021-89, especially for the positive bending moment. Most of the differences

range from 30% to 40%, and the maximum value is almost larger than 45%.

4.2. Four-Span Continuous Girder Bridges. The comparison results of the traffic loading effects of three-span continuous girder bridges without the dynamic load allowance are shown in Figure 10.

Figure 10(a) shows that the negative bending moment calculated based on JTG D60-2004 is smaller than that calculated based on JTJ 021-89 when the span length is less than 35 m, while the negative bending moment calculated based on JTG D60-2004 is larger than that calculated based on JTJ 021-89 when the span length is longer than 35 m. In addition, the positive bending moment calculated based on JTG D60-2004 is significantly larger than that calculated based on JTJ 021-89. The differences between them range from almost 10% to 20%.

Similarly, it can be seen from Figure 10(b) that the trend of the negative bending moment is almost the same as that in Figure 10(a). However, the positive bending moment

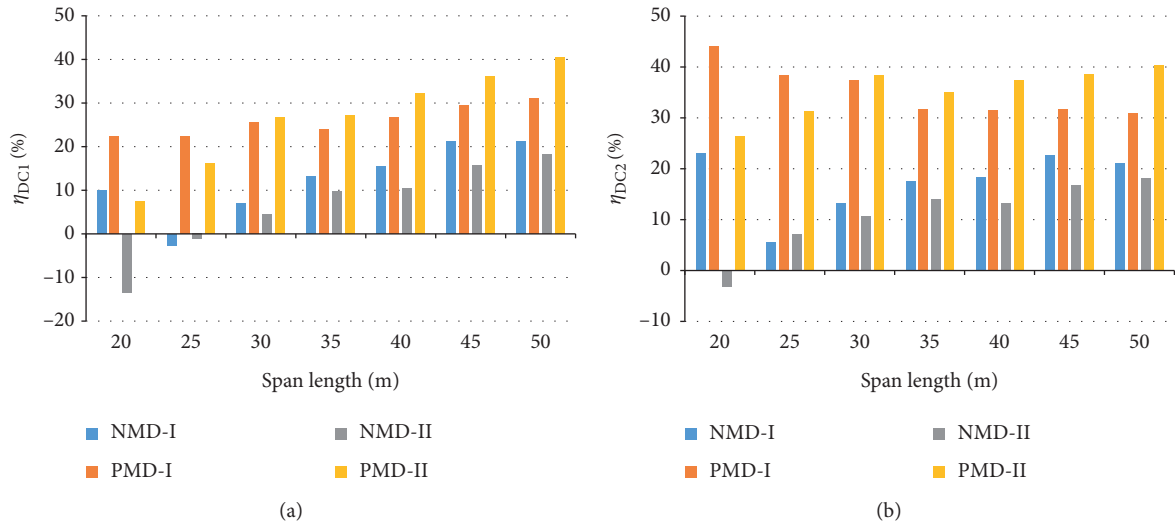


FIGURE 11: Comparison of the traffic loading effects of four-span continuous girder bridges with dynamic load allowance: (a) η_{DC1} and (b) η_{DC2} .

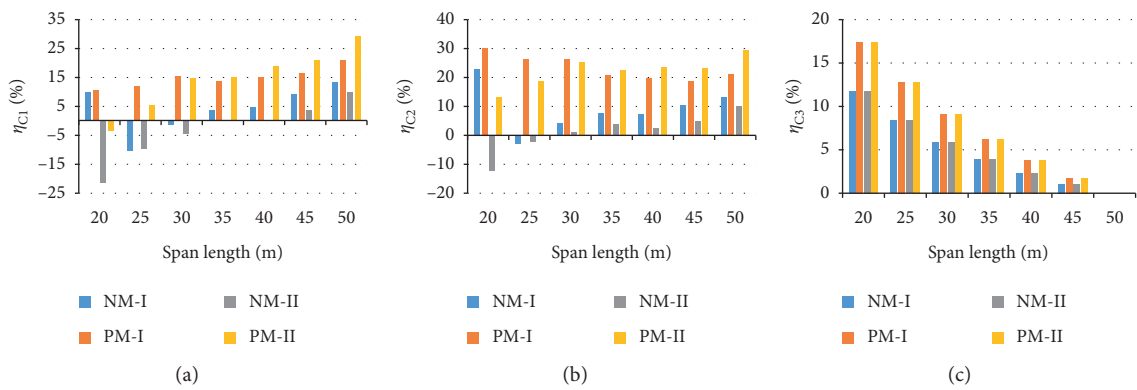


FIGURE 12: Comparison of the traffic loading effects of five-span continuous girder bridges without the dynamic load allowance: (a) η_{C1} ; (b) η_{C2} ; (c) η_{C3} .

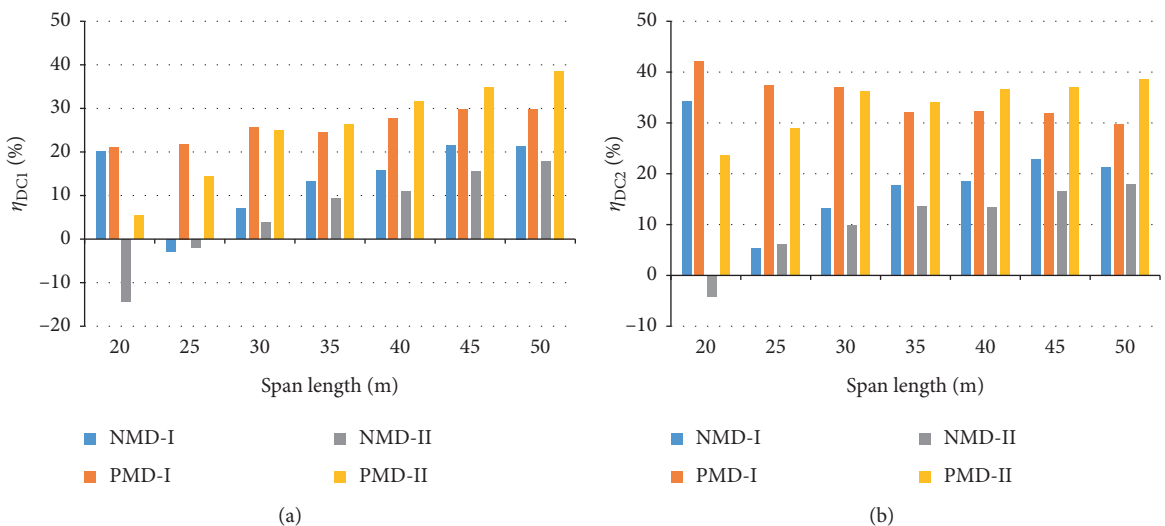


FIGURE 13: Comparison of the traffic loading effects of five-span continuous girder bridges with the dynamic load allowance: (a) η_{DC1} and (b) η_{DC2} .

calculated based on JTG D60-2004 is significantly larger than that calculated based on JTJ 021-89. Most of the differences range from 15% to 30%, and the largest difference is 32%.

In Figure 10(c), the comparison of the traffic loading effects between JTG D60-2004 and JTJ 021-89 is very regular because their traffic loading models are similar, and only the value of concentrated force P_k is different. The differences between these values decrease with increasing span length. For small-span continuous girder bridges, the difference can reach almost 18% and 12% for the positive bending moment and negative bending moment, respectively.

A comparison of the traffic loading effects of four-span continuous girder bridges with the dynamic load allowance in different codes is shown in Figure 11.

Figure 11(a) shows that, with the dynamic load allowance, the positive bending moments of four-span continuous girder bridges calculated based on JTG D60-2015 are significantly larger than those calculated based on JTJ 021-89. The differences in the positive bending moment are larger than 20%. In addition, the largest difference in the negative bending moment can reach 21%.

Similarly, it can be seen from Figure 11(b) that all the traffic loading effects of four-span continuous girder bridges calculated based on JTG D60-2015 are significantly larger than those calculated based on JTJ 021-89, especially for the positive bending moment. Most of the differences range from 30% to 40%, and the maximum value is almost 45%.

4.3. Five-Span Continuous Girder Bridges. The comparison results of the traffic loading effects of five-span continuous girder bridges without dynamic load allowance are shown in Figure 12.

Figure 12(a) shows that the negative bending moment calculated based on JTG D60-2004 is smaller than that calculated based on JTJ 021-89 when the span length is less than 35 m, while the negative bending moment calculated based on JTG D60-2004 is larger than that calculated based on JTJ 021-89 when the span length is longer than 35 m. In addition, the positive bending moment calculated based on JTG D60-2004 is significantly larger than that calculated based on JTJ 021-89. The differences between them ranged from almost 10% to 20%.

Similarly, it can be seen from Figure 12(b) that the trend of the negative bending moment is almost the same as that in Figure 12(a). However, the positive bending moment calculated based on JTG D60-2004 is significantly larger than that calculated based on JTJ 021-89. Most of the differences range from 15% to 30%.

In Figure 12(c), the comparison of the traffic loading effects between JTG D60-2004 and JTJ 021-89 is very regular because their traffic loading models are similar, and only the value of concentrated force P_k is different. The differences between them decrease with increasing span length. For small-span continuous girder bridges, the difference can reach almost 18% and 12% for the positive

bending moment and negative bending moment, respectively.

The comparison of the traffic loading effects of five-span continuous girder bridges with the dynamic load allowance in different codes is shown in Figure 13.

Figure 13(a) shows that, with dynamic load allowance, the positive bending moments of five-span continuous girder bridges calculated based on JTG D60-2015 are significantly larger than those calculated based on JTJ 021-89. The differences in the positive bending moment are larger than 10%. In addition, the largest difference in the negative bending moment can reach 21%.

Similarly, it can be seen from Figure 13(b) that all the traffic loading effects of five-span continuous girder bridges calculated based on JTG D60-2015 are significantly larger than those calculated based on JTJ 021-89, especially for the positive bending moment. Most of the differences range from 20% to 40%, and the maximum value is almost 42%.

In other words, for continuous girder bridges, the number of spans has only a small influence. The positive bending moment is much more sensitive than the negative bending moment with various codes. The positive bending moments calculated based on JTG D60-2004 and JTG D60-2015 are significantly larger than those calculated based on JTJ 021-89. Most of the differences in the positive bending moments are concentrated in the 20%~40% range. The differences in the negative bending moment range from 10% to 20%.

Of course, for continuous girder bridges, the differences in traffic loading effects calculated based on various codes cannot be ignored in actual bridge engineering, especially for the positive bending moments.

5. Conclusions

Traffic loading effects in different codes on medium- and small-span girder bridges in China are investigated in this study. Three codes are selected including JTJ 021-89, JTG D60-2004, and JTG D60-2015, and simply supported girder bridges and continuous girder bridges are discussed.

- (1) The traffic loading effects of simply supported girder bridges calculated based on JTG D60-2015 are significantly larger than those calculated based on JTJ 021-89, especially for small-span bridges. Most of the differences range from 20% to 40%, and the maximum value is almost larger than 60%.
- (2) For continuous girder bridges, the number of spans has only a slight influence. The positive bending moment is much more sensitive than the negative bending moment with various codes. The positive bending moments calculated based on JTG D60-2004 and JTG D60-2015 are significantly larger than those calculated based on JTJ 021-89. Most of the differences in the positive bending moments are concentrated in the 20%~40% range. The differences in the negative bending moment range from 10% to 20%.

Therefore, the differences in traffic loading effects calculated based on various codes cannot be ignored in actual bridge engineering.

Data Availability

The data used to support the findings of this study are included within the article.

Conflicts of Interest

The authors declare that they have no conflicts of interest.

Acknowledgments

This work was supported by the National Natural Science Foundation of China (51778194), the China Postdoctoral Science Foundation (2017M621282), and the Fundamental Research Funds for the Central Universities (HIT. NSRIF. 2019056).

References

- [1] Ministry of Transport of the People's Republic of China, "Statistical Bulletin on the Development of the Transport Industry in 2019," http://www.gov.cn/xinwen/2020-05/12/content_5510817.htm.
- [2] Q. Huang, J. Guan, C. Liang, T. Wang, and X. Wang, "Comparative study on vehicle loads and action effects of bridge design specifications of China, US and Europe," *Journal of Highway and Transportation Research and Development*, vol. 37, no. 7, pp. 62–71, 2020.
- [3] S. Zhang and Y. Liu, "Damage detection of bridges monitored within one cluster based on the residual between the cumulative distribution functions of strain monitoring data," *Structural Health Monitoring*, 2020.
- [4] X. Shi, B. Zhao, Y. Yao, and F. Wang, "Prediction methods for routine maintenance costs of a reinforced concrete beam bridge based on panel data," *Advances in Civil Engineering*, vol. 2019, Article ID 5409802, 12 pages, 2019.
- [5] Q. Gao, K. Cui, J. Li, B. Guo, and Y. Liu, "Optimal layout of sensors in large-span cable-stayed bridges subjected to moving vehicular loads," *International Journal of Distributed Sensor Networks*, vol. 16, no. 1, pp. 1–13, 2020.
- [6] S. A. Dabous and G. Al-Khayyat, "A flexible bridge rating method based on analytical evidential reasoning and Monte Carlo simulation," *Advances in Civil Engineering*, vol. 2018, Article ID 1290632, 13 pages, 2018.
- [7] Q. Gao, Z. Dong, K. Cui, and Y. Liu, "Fatigue performance of profiled steel sheeting-concrete bridge decks subjected to vehicular loads," *Engineering Structures*, vol. 213, Article ID 110558, 2020.
- [8] R. Wang, X. Ma, and J. Wang, "Comparison and analysis of automobile load of urban bridge with highway bridge," *Urban Roads Bridges & Flood Control*, vol. 5, pp. 154–157, 2006.
- [9] T. Wu, Y. Ge, J. Xiong, and X. Ye, "Development and comparison of vehicular loads on highway bridge in our country," *Shanghai Highways*, vol. 1, pp. 37–41, 2007.
- [10] X. Du, Y. Zhao, and J. Guo, "Discussion on live load on the bridge of outside mining area," *Shanxi Architecture*, vol. 34, no. 29, pp. 312–313, 2008.
- [11] P. Liang, T. Long, J. Qin, and S. Xiao, "Analysis on the load evolution and its effect of bridge vehicle in China," *Highway*, vol. 11, pp. 86–94, 2011.
- [12] S. Si, "Comparative study of the influence of highway bridge regulation on vehicle load effect of simply supported beam bridge," *Journal of Lanzhou Institute of Technology*, vol. 23, no. 5, pp. 13–17, 2016.
- [13] D. Qian, "Automobile load effect analysis based on the change of old and new bridge design specifications," *Engineering and Construction*, vol. 31, no. 1, pp. 24–26, 2017.
- [14] C. Mei, "Comparative analysis of traffic load analysis methods in old and new specifications," *Journal of China & Foreign Highway*, vol. 39, no. 1, pp. 291–295, 2019.
- [15] Z. Li and R. Chang, "Internal force analysis of continuous bridge due to different loads," *Journal of Hebei University of Technology*, vol. 38, no. 1, pp. 86–90, 2009.
- [16] L. Liu, Q. Ren, and X. Wang, "Calibration of the live load factor for highway bridges with different requirements of loading," *Advances in Civil Engineering*, vol. 2020, Article ID 7347593, 10 pages, 2020.
- [17] M. Ghosn and F. Moses, "Markov renewal model for maximum bridge loading," *Journal of Engineering Mechanics*, vol. 111, no. 9, pp. 1093–1104, 1985.
- [18] A. Nowak and Y. Hong, "Bridge live load models," *Journal of Structural Engineering*, vol. 121, no. 8, pp. 1245–1251, 1991.
- [19] F. Moses, "Weigh-in-motion systems using instrumented bridges," *Transportation Engineering Journal*, vol. 105, no. 3, pp. 233–249, 1979.
- [20] A. O'Connor and E. J. O'Brien, "Traffic load modelling and factors influencing the accuracy of predicted extremes," *Canadian Journal of Civil Engineering*, vol. 32, no. 1, pp. 270–278, 2005.
- [21] Ministry of Transport of the People's Republic of China, "General Specifications for Design of Highway Bridges and Culverts," JTJ 021-89.
- [22] Ministry of Transport of the People's Republic of China, "General Specifications for Design of Highway Bridges and Culverts," JTG D60-2004.
- [23] Ministry of Transport of the People's Republic of China, "General Specifications for Design of Highway Bridges and Culverts," JTG D60-2015.
- [24] Q. Gao, K. Zhang, C. Liu, Y. Sun, and Z. Li, "Discussions on the impact factor of bridges subjected to moving vehicular loads," *Journal of Harbin Institute of Technology*, vol. 52, no. 3, pp. 44–50, 2020.
- [25] L. Deng, Y. Yu, Q. Zou, and C. S. Cai, "State-of-the-art review of dynamic impact factors of highway bridges," *Journal of Bridge Engineering*, vol. 20, no. 5, Article ID 04014080, 2014.